Progress In Electromagnetics Research M, Vol. 2, 189–200, 2008

WAVELET-BASED MOMENT METHOD AND PHYSICAL OPTICS USE ON LARGE REFLECTOR ANTENNAS

M. Lashab

Département d'Électronique
Université du 20 Août 55
Skikda, Algeria

C. Zebiri

Département d'Électronique
Université de Sétif
Algeria

F. Benabdelaziz

Département d'Électronique
Université de Mentouri
Constantine, Algeria

Abstract—With the recent advent on communication and satellite industry, there is a great need for efficient Reflector antennas systems, therefore more powerful techniques are requested for analysis and design of new reflector antennas in a quick and accurate manner. This work aim first to introduce wavelet-based moment method in 3D, as a recent and powerful numerical technique, which can be applied on a large reflector antennas, also the physical optics (PO) analysis technique is well known among the designers as an asymptotic method quick and powerful, ideally to predict far field and near field pattern, may be combined with the wavelet-based moment method therefore computing time and memory space can be saved, in this issue knowing the limit of use of this asymptotic technique is worth well.

1. INTRODUCTION

Great research works are undergoing to develop new schemes for analysis and design of better reflector antennas more efficiently and accurately. This paper presents a recent improvement on the classical moment method, which suffers from computing time and memory space, especially when dealing with large antennas. By using the wavelets expansion, wavelets may be used as basis and testing functions, wavelets are chosen as orthogonal types, in order to enable sparse the matrix impedance generated by the operation digitalization of the integral equation of the electric or magnetic field. Many research work have curried out to apply wavelets on electromagnetic scattering problems [4], some have been used upon 2D scattering problems [6, 9, 13]. Few works were using wavelets upon 3D scattering problems from conducting bodies of revolution [12].

A great Work have been done on the asymptotic Physical Optics techniques some have upgrade this method by replacing the surface current integration with the so called numerical grid integration [3, 8, 10]. Others have combined the (OP) with the moment method [5, 7]. The work presented by Y. R. Samii [1] some Anomalous of the Optical Physics have been stated and care must be taken when using this technique for the far field pattern. In this paper the Optical Physics is applied on a simple reflector antennas fed by a short dipole antenna, results are compared with the wavelets-based moment method and the Grasp software in order to limit the use of this technique.

The paper is presented as follow, first the theoretical aspect of the Physical Optics is presented and applied on the reflector antenna in brief way, second the wavelet-based moment method is given in detail to study the 3D scattering problem and applied upon the reflector antenna, at last the radiation pattern of co-polarization and cross-polarization are given and the numerical results are discussed.

2. FORMULATION

2.1. Optical Physics

The radiation pattern for far field related to the reflector antenna shown in Figure 1, is given by the integral equation as [2].

$$\vec{E}_{ray}\left(\theta', \phi'\right) = -jkZo\frac{e^{-jk|\vec{r}'|}}{|\vec{r}'|}\left(\tilde{I} - \hat{r}'\hat{r}'\right)\iint_S \bar{J}_s e^{jk.\vec{r}\hat{r}'} ds \qquad (1)$$

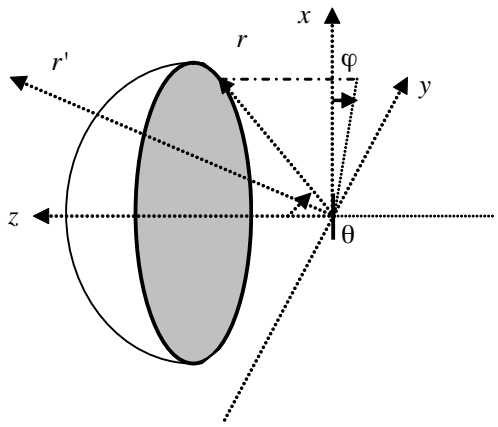

Figure 1. Reflector antenna fed by a dipole antenna.

where the primed quantities are related to the radiation pattern coordinate and the not primed are related to the reflector coordinate Figure 1, k is the free space propagation and Zo is the intrinsic impedance of free space, $\tilde{I}$ is the unit dyadic and $\bar{J}_s$ is the induced surface current. The surface of the reflector antenna is considered to be perfectly conductor (PEC), this is illustrated by the following equation.

$$J_S = \hat{n} \times \left(\vec{H}_i + \vec{H}_r\right) = 2\hat{n} \times \vec{H}_i \tag{2}$$

where $\hat{n}$ is the unit normal vector to the reflector surface, the electric field coming from the feed antenna is given in terms of principle plane pattern as [11].

$$\vec{E}_{inc}\left(\vec{r}_s\right) = \left[\left(C_E(\theta_s)\sin(\varphi_s)\right)\hat{\theta}_s + \left(C_H(\theta_s)\cos(\varphi_s)\right)\hat{\varphi}_s\right]\frac{e^{-jk.r_s}}{r_s} \tag{3}$$

The index (s) refers to the source coordinate in case where the source is displaced for an offset reflector, and $C_E(\theta s)$, $C_H(\theta s)$ define the E-plane and the H-plane principal patterns respectively, defined as

$$C_E(\theta_s) = \cos^{qe}(\theta_s) \tag{4}$$

$$C_H(\theta_s) = \cos^{qh}(\theta_s) \tag{5}$$

The constants qe and qh serves to define the principal E and H planes. The magnetic incident field is deduced by the following

relation.

$$\vec{H}_{inc}\left(\vec{r}_s\right) = \frac{1}{Zo}\vec{r}_s \times \vec{E}_{inc}\left(\vec{r}_s\right) \tag{6}$$

The reflector is considered to be parabolic, the surface is then defined by following relation

$$r = \frac{2Fo}{1+\cos\theta} \tag{7}$$

where Fo is the focal distance, from Equation (7) the normal vector to the surface and the unit normal vector can be written respectively as

$$\vec{n} = -(1+\cos\theta)\hat{r} + (\sin\theta)\hat{\theta} \tag{8}$$

$$\hat{n} = \frac{\vec{n}}{|\vec{n}|}$$

The radiation pattern for the far field Equation (1), is expressed more by the following expression as

$$\vec{E}_{ray}(\theta', \phi') = -jkZo\frac{e^{-jk|\vec{r}'|}}{|\vec{r}'|}\left[F - \hat{r}'(\hat{r}\,'.F)\right] \tag{9}$$

where F is given by

$$F = \int_0^{2\pi}\int_0^{\theta_o} J_s.e^{jk.\vec{r}.\hat{r}'}r^2\sec(\theta/2)\sin(\theta)d\theta.d\varphi \tag{10}$$

where θ_o is the maximum open angle on the reflector, the induced surface current is defined by replacing Equation (6) into (2), after then the electric radiation pattern is obtained from Equation (9). All the research works curried out on the asymptotic Optical physics are dealing with the integral part.

2.2. Wavelet-based Moment Method

2.2.1. Integral Equation

Moment Method is based on discritization of the electric integral equation (EFIE), for the problem geometry of Figure 1, this is defined as [2].

$$\vec{E}_{inc}(r) = \frac{j}{\varepsilon_0\omega}\int_S \left[k^2 J\left(r'\right).G\left(r,r'\right) + \nabla' J\left(r'\right).\nabla G\left(r,r'\right).\right]dS' \tag{11}$$

where $G(r, r')$ is the free space green's function:

$$G\left(r, r'\right) = \frac{e^{-jk|r-r'|}}{4\pi.\left|r-r'\right|} \tag{12}$$

The boundary condition applied on the perfect surface of the reflector antenna can be expressed as

$$\vec{E}_{inc} + \vec{E}_r = 0 \tag{13}$$

The density of current is expressed by two tangential components on the surface of the reflector as follow.

$$J(t, \varphi) = J_t(t, \varphi).\hat{u}_t + J_\varphi(t, \varphi).\hat{u}_\varphi \tag{14}$$

Each component is expressed as the sum of $N \times M$ series of functions on the surface of the reflector as [12].

$$J_t(t, \varphi) = \sum_{n=1}^{N} \sum_{m=1}^{M} I_{n,m}^t b_n^t(t, \varphi).e^{jn.\varphi} \tag{15}$$

And

$$J_\varphi(t, \varphi) = \sum_{n=1}^{N} \sum_{m=1}^{M} I_{n,m}^\varphi b_n^\varphi(t, \varphi).e^{jn.\varphi} \tag{16}$$

where $b_n^t(t, \varphi)$ and $b_n^\varphi(t, \varphi)$ are the basis functions, and $I_{n,m}^t$, $I_{n,m}^\varphi$ are the unknowns. Using the boundary condition (13) in the integral Equation (11), the scattered field can be expressed as follow

$$E_{scat}(t, \varphi) = \int_0^{2\pi} \int_0^{R_{\max}} L\left(J_t, J_\varphi\right) d\varphi dt \tag{17}$$

where $R_{\max}$ is the maximum arclength of the generating curve, and $L(J_t, J_\varphi)$ is a differential operator defined as:

$$L\left(J_t, J_\varphi\right) = \frac{j}{\varepsilon_o \omega}\left(\frac{\partial}{\partial\varphi.\partial t} + k^2 \hat{t}.\hat{\varphi}\right) J\left(t', \varphi'\right).G\left(r, r'\right) r'(t) \tag{18}$$

For the sake of simplicity and for later use, Equation (17) is written as

$$T(t, \varphi) = \int_0^{2\pi} \int_0^{R\max} L\left(J_t, J_\varphi\right) d\varphi dt \tag{19}$$

2.2.2. Wavelets Expansions

The basis and testing functions are presented as a superposition of wavelets at several scales including the scaling function. A Galerkin method is then applied, where the set of basis functions used to present the current function, are used as weighting functions. The wavelets used here are Haar basis an orthogonal type. Its study is useful from theoretical point of view, because it offers an intuitive understanding of many multi-resolution properties. Furthermore, due to its simplicity Haar wavelets are widely employed. The scaling function is $\phi(x)$, and the mother wavelet function is $\psi(x)$ [4], these are defined as:

$$\phi_{jn}(x) = 2^{j/2}\phi\left(2^j x - n\right) \tag{20}$$

And

$$\psi_{mn}(x) = 2^{m/2}\psi\left(2^m x - n\right) \tag{21}$$

where (m or j) are the resolution level and (n) is the translation factor. The vector space V^j linear span of ϕ_{jn} for $j = 0, 1, \ldots$ And $n = 0, 1, \ldots, 2^j - 1$. The vector space W^j linear span of ψ_{jn} for $j = 0, 1, \ldots$. And $n = 0, 1, \ldots, 2^j - 1$. The property of $W^j \subseteq V^{j+1}$ holds the relation between the vector spaces of different functions by:

$$V^{j+1} = V^j \oplus W^j \tag{22}$$

The above equation states that the subspace W^j is the orthogonal complement of V^j in a larger subspace V^{j+1}, which means for a given function $f \in R^N$ with N samples or N Dimensional vector, the projection of this function into the orthogonal basis is as fellow:

$$V^k = V^0 \oplus W^0 \oplus W^1 \ldots \oplus W^{k-1}, \quad k = 0, 1, \ldots, N-1 \tag{23}$$

And can be expressed in inner product as:

$$f = \langle f, v_0\rangle v_0 + \langle f, v_1\rangle v_1 + \ldots + \langle f, v_{N-1}\rangle v_{N-1} \tag{24}$$

The number of wavelets used here are 128 and the matrix corresponding is of $128 \times 128 = 16384$ elements. Some of these wavelets are represented in Figure 2 and Figure 3.

A function $\psi(x)$ is said to have vanishing moment of N order if:

$$\int_{-\infty}^{+\infty} x^n.\psi(x).dx = 0 \quad \forall n = 0, 1, \ldots, (N-1) \tag{25}$$

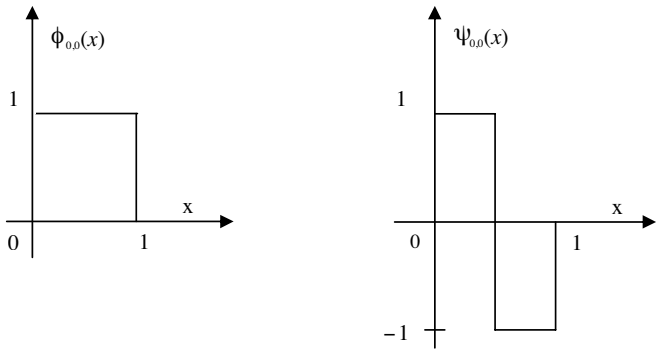

Figure 2. Haar wavelets $\phi_{0,0}$ and $\psi_{0,0}$.

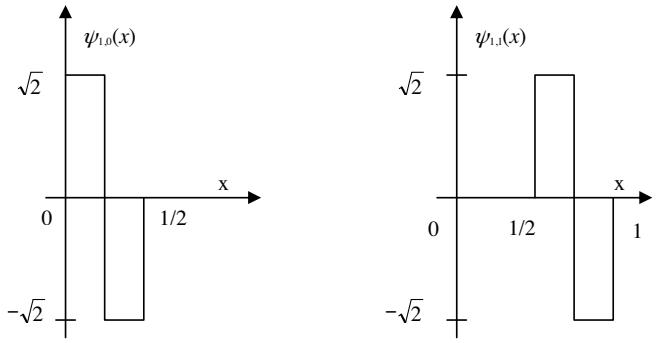

Figure 3. Haar wavelets $\psi_{1,0}$ and $\psi_{1,1}$.

The wavelets are applied directly upon the integral equation. The density of current will be represented as a linear combination of the set wavelets functions and scaling functions as fellow:

$$J_t(t,\varphi) = \sum_{n=0} a_n^t . \phi_{j.n}^t(t,\varphi) + \sum_{m=j}^{2^j-1} \sum_{n=0} c_{m.n}^t \psi_{m.n}^t(t,\varphi) \qquad (26)$$

And

$$J_\varphi(t,\varphi) = \sum_{n=0} a_n^\varphi . \phi_{j.n}^\varphi(t,\varphi) + \sum_{m=j}^{2^j-1} \sum_{n=0} c_{m.n}^\varphi \psi_{m.n}^\varphi(t,\varphi) \qquad (27)$$

For the sake of simplicity the current density is expressed only by the

scaling functions as

$$J_t = \sum_n I_t \phi_n^t \tag{28}$$

And

$$J_\varphi = \sum_n I_\varphi \phi_n^\varphi \tag{29}$$

The fact that the wavelets are orthogonal and the presence of vanishing moment, this is enabling sparse matrix production. When applying Equations (28) and (29) into (19), we obtain the set of matrix equation as follow:

$$\begin{bmatrix} Z_{k,l}^{t,t} & Z_{k,l}^{t,\varphi} \\ Z_{k,l}^{\varphi,t} & Z_{k,l}^{\varphi,\varphi} \end{bmatrix} \cdot \begin{bmatrix} I_l^t \\ I_l^\varphi \end{bmatrix} = \begin{bmatrix} E_k^t \\ E_k^\varphi \end{bmatrix} \tag{30}$$

where each element of the matrix is double inner product from the wavelets functions in two coordinate as

$$Z_{k,l}^{t,t} = \langle \phi_k, \langle \phi_l, T(t,t).\Omega(r,\xi) \rangle \rangle \tag{31}$$

where $\Omega(r,\xi)$ is the changing variable operator from r to ξ, here ξ is the variable related to wavelet in the domain [0, 1]. Equation (31) is written in explicit manner as [12].

$$Z_{k,l}^{t,t} = \int_0^1 \phi_k \left[\int_0^1 \phi_l \; T(t,t) \; \Omega(r,\xi) \; d\xi \right] d\xi' \tag{32}$$

In the same manner the remaining elements are expressed as follow

$$Z_{k,l}^{t,\varphi} = \langle \phi_k, \langle \phi_l, T(t,\varphi).\Omega(r,\xi) \rangle \rangle \tag{33}$$

$$Z_{k,l}^{\varphi,t} = \langle \phi_k, \langle \phi_l, T(\varphi,t).\Omega(r,\xi) \rangle \rangle \tag{34}$$

$$Z_{k,l}^{\varphi,\varphi} = \langle \phi_k, \langle \phi_l, T(\varphi,\varphi).\Omega(r,\xi) \rangle \rangle \tag{35}$$

The excitation in the matrix Equation (30) is expressed as an inner product of testing functions by

$$E_k^t = \left\langle \phi_k, E_{inc}^t \right\rangle \tag{36}$$

$$E_k^\varphi = \langle \phi_k, E_{inc}^\varphi \rangle \tag{37}$$

After then the matrix Equation (30) is solved and the unknowns $([I^t, I^\varphi])$ are defined, which enable radiation patterns calculation.

3. NUMERICAL RESULTS

The wavelets used in this paper are constructed from Haar, an orthogonal type with vanishing moment $N = 7$, the lowest resolution level is chosen $2^j = 2^7 = 128$, since 128 wavelets are involved, a system of matrix (of 128×128 elements) is generated.

The radiation patterns of the E-plane and H-plane for co-polarization are presented respectively in Figure 4 and Figure 5, for $F/D = 0.6$, $D = 100\lambda$, $qe = qh = 4.9$, incident angle $\varphi = 90°$. The results show good agreement with Grasp Software, and Physical Optics gives the main lobe and second one exactly as presented. The results presented are for co-polarisation only and there is no cross polarisation.

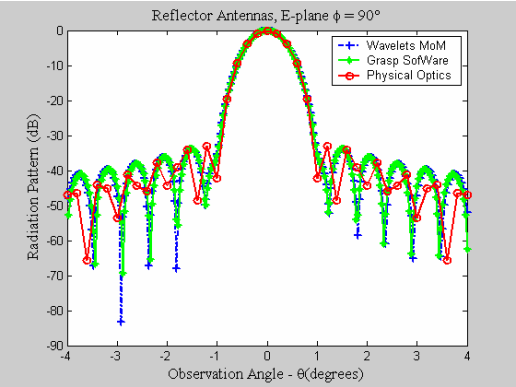

Figure 4. E-plane radiation pattern for parabolic reflector fed by dipole antenna, $F/D = 0.6$, $D = 100\lambda$, $qe = qh = 4.9$, $\varphi = 90°$.

Butter result are obtained for the physical optics when using high value of $F/D = 0.8$, Figure 6 and Figure 7 show the radiation pattern respectively for E-plane and H-plane, here the cross-polarization is higher with $\varphi = 45°$.

The resolution of the wavelets is set to 2^7 for threshold of 10^{-3} a sparsity of 78% is obtained, going for upper resolution enable accurate results but the impedance matrix became very heavy, so a compromise have to be done, the results are in good agreement with the Grasp software and with literature. The sparsification of the impedance matrix with respect to the chosen threshold and the wavelet number is presented in Table 1.

One can notice from the Table 1, that increasing wavelet number can improve sparsification and lower threshold decrease sparsification. Although accuracy of the results are obtained for very low threshold a compromise is necessary.

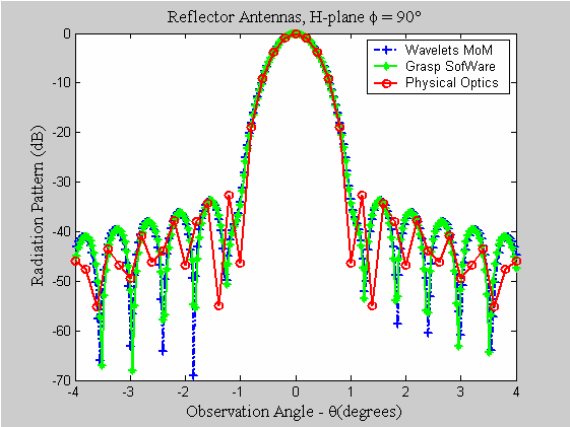

Figure 5. H-plane radiation pattern for parabolic reflector fed by dipole antenna, $F/D = 0.6$, $D = 100\lambda$, $qe = qh = 4.9$, $\varphi = 90°$.

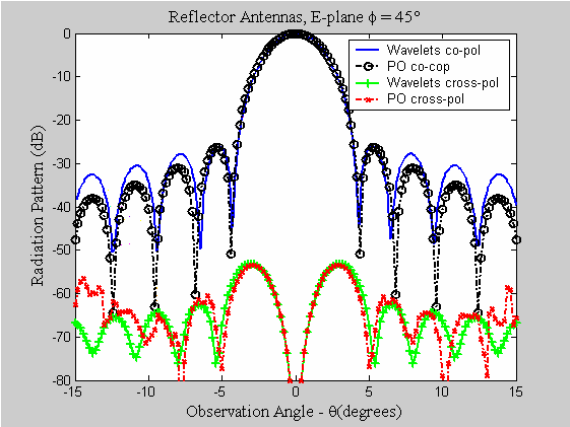

Figure 6. E-plane radiation pattern for parabolic reflector fed by dipole antenna, $F/D = 0.8$, $D = 20\lambda$, $qe = qh = 6.5$, $\varphi = 45°$.

Table 1. Sparsification with respect to the threshold and the wavelet number.

Threshold	10^{-2}				10^{-3}				10^{-4}			
Wavelet Number	32	64	128	512	32	64	128	512	32	64	128	512
Sparsity (%)	79.50	85.11	89.34	91.03	63.41	75.33	78.12	80.56	58.22	68.02	71.23	73.05

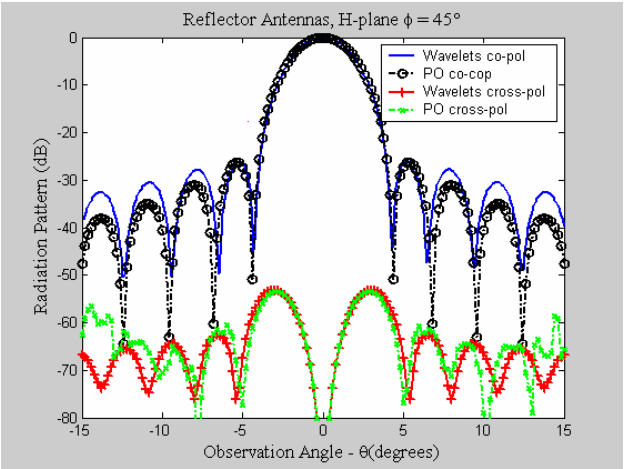

Figure 7. H-plane radiation pattern for parabolic reflector fed by dipole antenna, $F/D = 0.8$, $D = 20\lambda$, $qe = qh = 6.5$, $\varphi = 45°$.

4. CONCLUSIONS

The Physical Optics asymptotic technique has been presented as well as the Wavelet-based Moment Method for the study of electromagnetic scattering related to the reflector antenna fed by a dipole antenna. In different cases it has show that the wavelet-based Moment Method is an exact and quick Method, results are similar to those given by Grasp software, and results of the Physical Optics are exact for main lobe for low F/D, and gives the second or the third lobe for high F/D, it has been noticed that excessive computing time is needed for higher value of D ($\exp .D = 100\lambda$). For a future work the Physical Optics may be used in combination with the Wavelet-based Moment Method for saving time and memory space.

REFERENCES

1. Rahmat-Samii, Y. and W. A. Imbriale, "Anomalous results from PO applied to reflector antennas: The importance of near field computations," *IEEE Trans. Antennas Propagat.*, Vol. 45, No. 4, 816–821, Aug. 1998.
2. Balanis, C. A., *Antennas Theory, Analysis and Design*, John Wiley & Sons, Inc., New York, 1997.
3. Bibi, S. and N. Faisal, "Analysis side lobe reflector antennas,"

IEEE Trans. Antennas & Propagat. Vol. 15, No. 6, 383–388, March 2006.

4. Pan, G. W., *Wavelet in Electromagnetics and Device Modeling*, John Wiley & Sons Publication, 2001.
5. Tap, K. and P. H. Pathak, "A fast hybrid asymptotic and numerical physical optics analysis of very large scanning cylindrical reflectors with stacked linear array feeds," *IEEE Trans. Antennas & Propagat.*, Vol. 54, No. 4, 212–218, Apr. 2006.
6. Anyutia, A. P. and A. G. Kyurkchan, "Application of the wavelets in 2D and 3D scattering for radiation problems," *IEEE Trans. Antennas & propagat.*, Vol. 15, No. 25, 452–457, Nov. 2003.
7. Moumen, A. and L. P. Ligthart, "A hybrid physical optics-moment method for reflector antennas with complex struts geometry and off-axis feeding," *IEEE Trans. Antennas & Propagat.*, Vol. 9, No. 31, 830–835, June 2000.
8. Obmaki, N. and L. Rodriguez, "Accuracy check of the PO with the modified surface-normal vectors for radar cross section analyses," *EMTS 2007 — International URSI Commission B — Electromagnetic Theory Symposium*, Ottawa, ON, Canada, July 26–28, 2007.
9. Lashab, M., F. Benabdelaziz, and C. Zebiri, "Analysis of electromagnetics scattering from reflector and cylindrical antennas using wavelet-based moment method," *Progress In Electromagnetics Research*, PIER 76, 357–368, 2007.
10. Arias, A. M. and A. M. E. Lorenzo, "A novel fast algorithm for physical optics analysis of single and dual reflector antennas," *IEEE Trans. on Magnetics*, Vol. 32, No. 3, 910–915, May 1996.
11. Herben, M. H. A. J. and M. M. J. L. van de Kamp, "Axial cross-polarization in reflector antennas due to asymmetric cross-polar feed patterns," *International Journal of Infrared and Millimeter Waves*, Vol. 9, No. 2, 1988.
12. Wang, G., "Analysis of electromagnetic scattering from conducting bodies of revolution using orthogonal wavelets expansions," *IEEE Trans. Electromag. Compabil.*, Vol. 40, No. 1, 1–11, Feb. 1998.
13. Vipiana, F., G. Vicchi, and M. Sabbadini, "A far field wavelet expansion for the synthesis of contoured-beam array-fed reflector antennas," *IEEE Trans. Antennas & Propagat.*, Vol. 11, No. 32, 589–593, July 2006.